Expert Systems with Applications 42 (2015) 1816–1824

Contents lists available at ScienceDirect

Expert Systems with Applications

journal homepage: www.elsevier.com/locate/eswa

Real-time illumination invariant lane detection for lane departure warning system

Jongin Son [a], Hunjae Yoo [a], Sanghoon Kim [b], Kwanghoon Sohn [a,*]

[a] The School of Electrical and Electronic Engineering, Yonsei University, Seoul 120-749, Republic of Korea
[b] Department of Broadcasting and Video, Cheju Halla University, Jeju, Republic of Korea

ARTICLE INFO

Article history:
Available online 25 October 2014

Keywords:
Lane detection
Driver assistance
Hough transform
LDWS
LKS

ABSTRACT

Lane detection is an important element in improving driving safety. In this paper, we propose a real-time and illumination invariant lane detection method for lane departure warning system. The proposed method works well in various illumination conditions such as in bad weather conditions and at night time. It includes three major components: First, we detect a vanishing point based on a voting map and define an adaptive region of interest (ROI) to reduce computational complexity. Second, we utilize the distinct property of lane colors to achieve illumination invariant lane marker candidate detection. Finally, we find the main lane using a clustering method from the lane marker candidates. In case of lane departure situation, our system sends driver alarm signal. Experimental results show satisfactory performance with an average detection rate of 93% under various illumination conditions. Moreover, the overall process takes only 33 ms per frame.

1. Introduction

Lane detection is an interesting and important research area for intelligent vehicle technologies because the number of car accident victims has increased annually with the growing number of vehicles on the road. Many accidents are caused by a lack of awareness about driving conditions due to driver carelessness or visual interference. Consequently, advanced driver assistance systems (ADAS) are regarded as an important technology to reduce the frequency of such accidents, and lane detection and tracking are considered to be basic modules for ADAS. ADAS uses a variety of sensors such as vision, scanning laser radar, radar, and global positioning system (GPS) devices. The research focuses on a vision-based application because vision sensors are cheaper than other sensors, and the performance of lane detection is superior (Youchun & Rongben, 2001). Vision-based methods such as inverse perspective mapping, particle filters, and Hough transforms (Graovac & Goma, 2012; Mccall & Trivedi, 2006; Southhall & Taylor, 2001) have been proposed for lane departure warning systems (LDWS) and lane keeping systems (LKS); however, they exhibit high computational complexities and unsatisfactory performances under various illumination conditions.

In this paper, we propose an illumination invariant lane detection algorithm which works well in various illumination conditions such as in bad weather conditions and at night time. It also works in real-time by reducing computational complexities to cope with rapidly changing traffic conditions. The main contributions of this paper can be summarized as follows:

- Robustness under various illumination conditions: We analyzed the invariance property of lanes under various illumination conditions, and used it to detect lanes. The proposed method also works well even under outdoor environment which diversely changes depending on the weather conditions and time.
- Low computational complexity: The proposed method defines an adaptive region of interest (ROI) by detecting a vanishing point and it creates a binary lane candidate image to reduce the computational complexity.

We tested our proposed lane detection algorithm for various experimental datasets to verify its performance. This study includes simulation results for datasets of 10236 frames from DIML-dataset1 (vehicular camera), DIML-dataset2 (smart phone camera), Caltech and SLD-2011 datasets.

This paper is organized as follows: Section 2 briefly reviews related works on lane detection systems. Section 3 describes a proposed lane detection system. Section 4 shows the details of the

* Corresponding author. Tel.: +82 2 2123 2879.
E-mail addresses: go3son@yonsei.com (J. Son), gnswo0112@yonsei.ac.kr (H. Yoo), shkim0207@gmail.com (S. Kim), khsohn@yonsei.ac.kr (K. Sohn).

http://dx.doi.org/10.1016/j.eswa.2014.10.024
0957-4174/

experimental environment and results. Finally, Section 5 provides the conclusion including further research suggestions.

2. Related works

Various studies have been done to detect and extract lanes using vision sensors. Most lane detection methods use the following three steps: The first one typically uses basic features such as edge, gradient and intensity (Borkar, Hayes, & Smith, 2012; Kong, Audibert, & Ponce, 2010; Wang, Lin, & Chen, 2010). Edges are one of the most significant features because lanes create strong edges on the road. In other words, large gradients exist between the road and lane due to the difference in their intensities. For example, edges of driving input image are extracted by canny edge detector (Cannny, 1986). The Hough transform (Southhall & Taylor, 2001) is then used to find straight line in the edge image which could be road lane. In addition, the modified Hough transform methods have been proposed for much quicker and enhanced memory efficiency (Kuk, An, Ki, & Cho, 2010; Leandro & Manuel, 2008). However, methods based on edge and Hough transform have many problems in detecting curved lanes, sensitivity in various illumination conditions, artifact and road patterns (Hsiao, Yeh, Huang, & Fu, 2006; Sotelo, Rodriguez, Magdalena, Bergasa, & Boquete, 2004). Gradient-enhancing conversion method was proposed to detect lane boundaries under various illumination conditions (Yoo, Yang, & Sohn, 2013). However, it does not work well in extremely different multi-illumination conditions such as water reflection in heavy rainfall at night because they assume that one scene does not include multiple illuminations.

The second method uses geometric information (David, Jose, Pablo, & Mateo, 2012). The geometric coordinate of camera and road lane have parameters that predict the detection of lanes (David et al., 2012). These parameters are used for Kalman and particle filters (Graovac & Goma, 2012). A new method using dynamic homography matrix estimation has been introduced recently for lane detection (Kang, Lee, Hur, & Seo, 2014). They showed good lane detection performance since parameters include the actual geometric information. However, it is not easy to define geometric information because the camera shakes and road environment frequently changes.

The last one uses lane color information. Vision-based methods usually convert RGB to HSI or custom color spaces because RGB color space is difficult to express the lane color information (Chin & Lin, 2005; Sun, Tsai, & Chan, 2006). In these alternate color spaces, the luminance and chrominance components of a pixel are separately modeled. As a result, the effects of shadows and various illumination conditions in color components can be greatly reduced. However, since these approaches operate at a pixel level, they are very sensitive to street lights or similar illumination sources. It is difficult to detect lanes in various environments such as road patterns and illumination conditions. Moreover, real-time processing is required to prevent accidents in an environment of fast driving. However, existing methods still have high computational complexities and unsatisfactory performances under various illumination conditions. We propose a new system which is fast and powerful in various illumination conditions without geometry information such as characteristics of the device and road environment.

3. Proposed method

Fig. 1 illustrates the overall process of the proposed system. Our proposed lane detection algorithm consists of 3 stages such as a vanishing point detection stage,a lane marker detection stage, and a lane clustering and fitting stage. First of all, we detect a vanishing point using a voting map to establish an adaptive ROI, which reduces the computational complexity at the vanishing point detection stage. Then, we obtain a binary lane image from the white and yellow lanes since typical road images include these lanes, and they retain their own properties of colors under various illumination conditions at the lane marker detection stage. Third, we detect main lanes using a clustering and fitting method in the binary lane image at the lane clustering and fitting stage. Finally, Our system determines that the lane departure situation based on finding main lane at the lane departure warning stage.

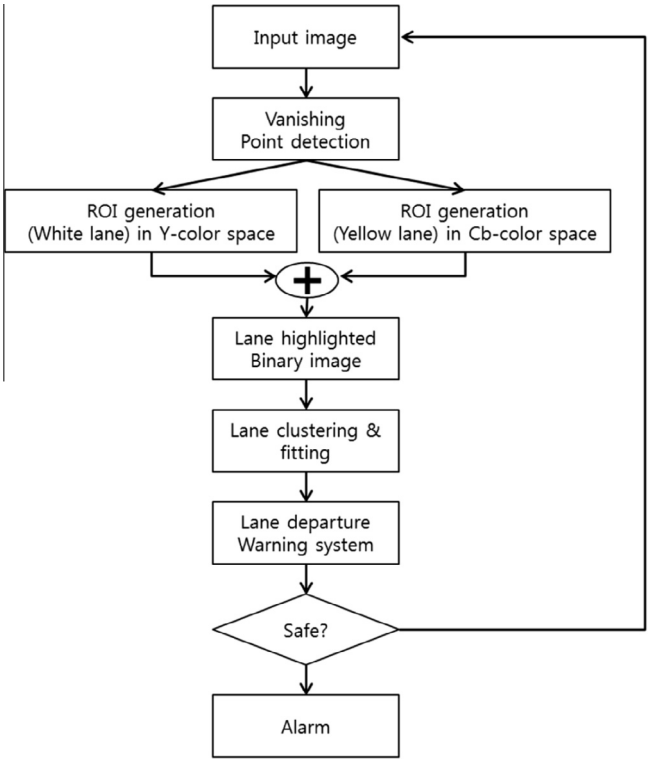

Fig. 1. Flowchart of the proposed lane detection algorithm.

3.1. Vanishing point detection stage

Lanes generally exist at the bottom half of a captured image while regions including the sky and landmarks appear at the top half (Foedisch & Takeuchi, 2004; Glaser, Mammar, & Sentouh, 2010). Thus, it is reasonable to consider only the bottom half of the image to extract the lane markings. However, the bottom half of the image may not be sufficient for lane detection because the features of those lane markings may be unclear and easily affected by illumination changes, shadows, and occlusions. Establishing an adaptive ROI using a vanishing point effectively reduces the computational complexity. In this paper, the vanishing point is detected as follows: First, edge detection preserves the structural properties important and significantly reduces the amount of data. Among the edge detection algorithms, we use the canny edge detector since it is robust to noise. In addition, we extract line components using Hough transform to use straight properties of lane. We detect line components using a canny edge detector and Hough transform as shown in Fig. 2(c) and (d). Second, we calculate the intersection point of the detected lines. Then, we generate a voting map which is cumulative line component sets. We counted the number of intersection points in voting map as shown in Fig. 2(e) and (f). Finally, we find the center point of the most voted area, which is defined as a vanishing point; it is denoted with a

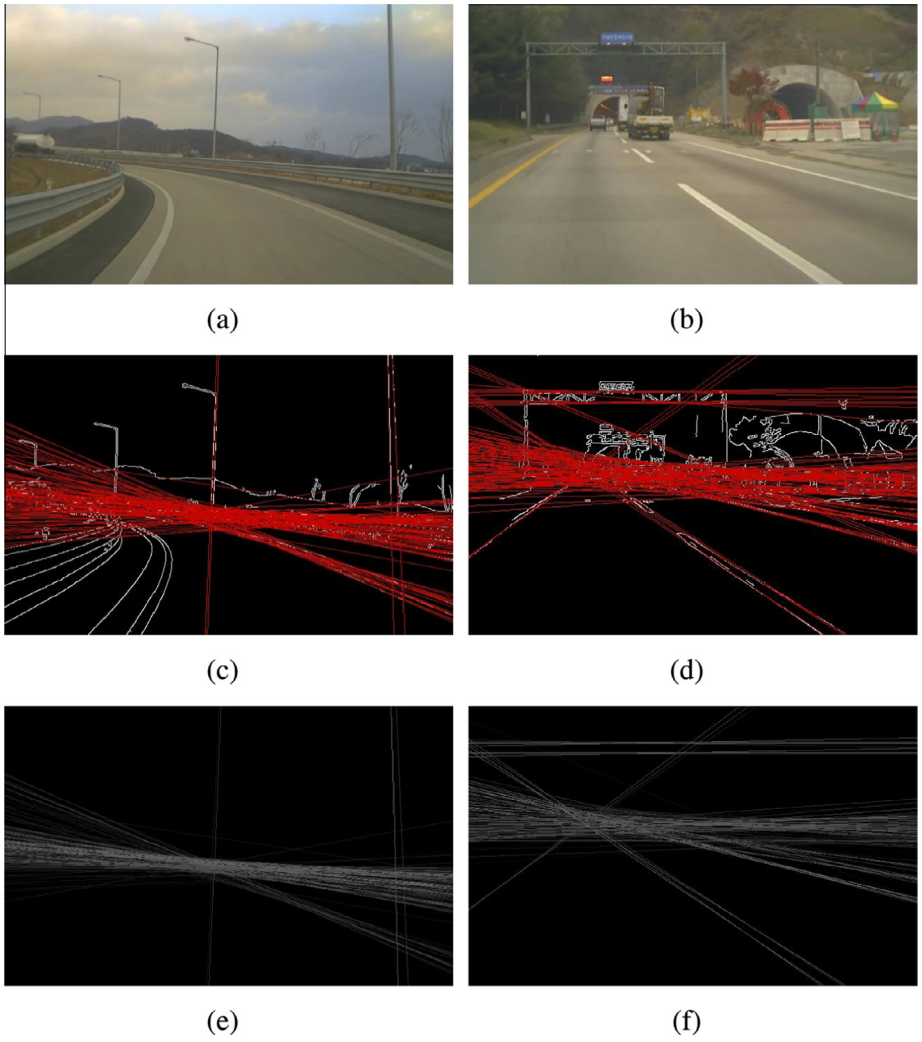

Fig. 2. Line component detection: (a) original image-1, (b) original image-2, (c) lines of image-1 extracted by hough transform, (d) lines of image-2 extracted by hough transform, (e) voting map for image-1 and (f) voting map for image-2.

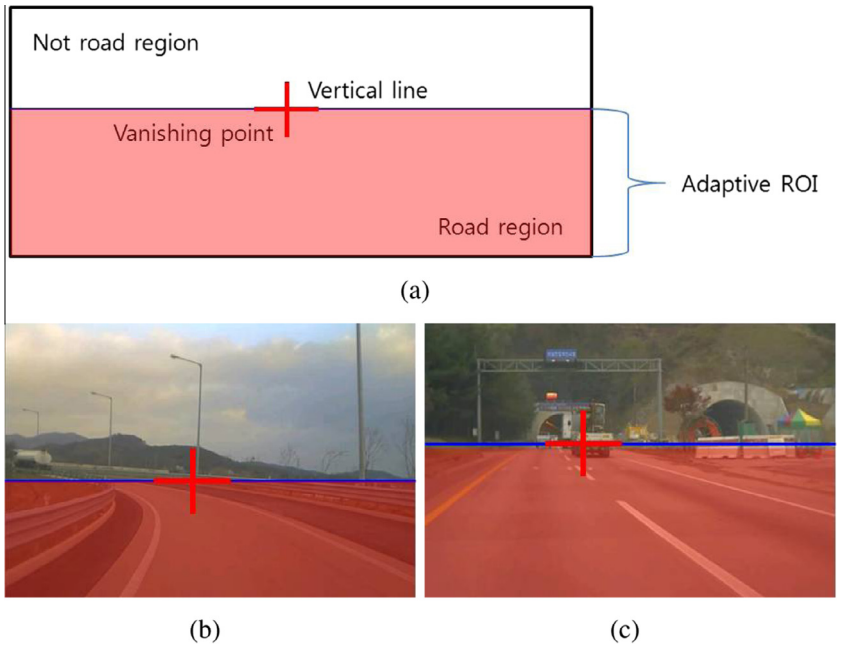

Fig. 3. Vanishing point detection: (a) scene layout of road image, (b) adaptive ROI of original image-1 and (c) adaptive ROI of original image-2.

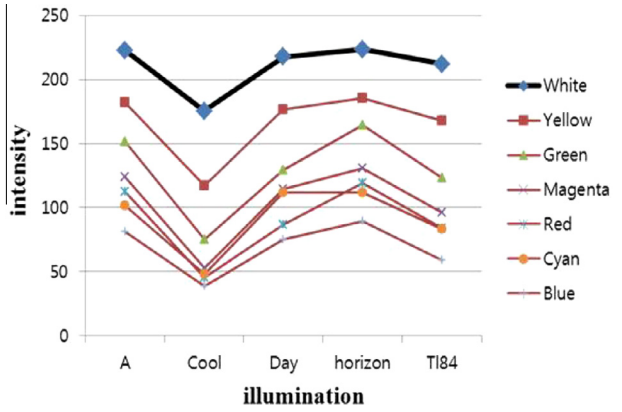

Fig. 4. Y-component values of representative colors under various illumination conditions. (For interpretation of the references to color in this figure legend, the reader is referred to the web version of this article.)

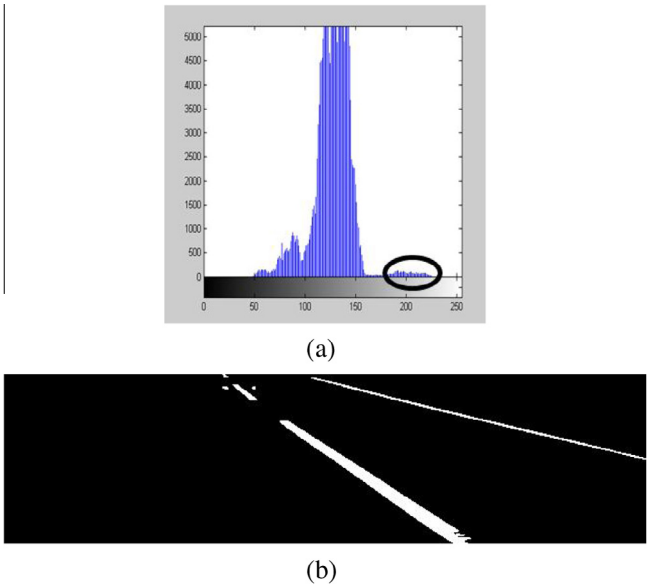

Fig. 5. White lane marker detection: (a) histogram for Y-component and (b) candidate of white lane marker regions.

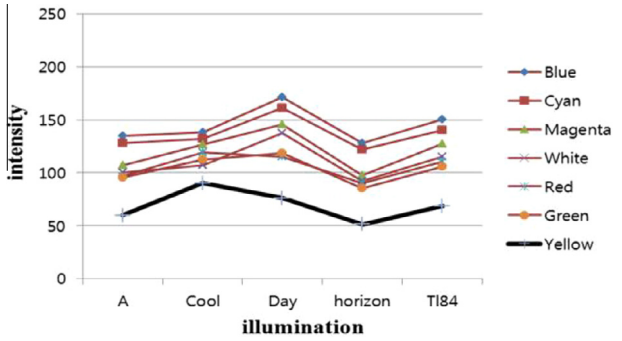

Fig. 6. Cb-component values of representative colors under various illumination conditions. (For interpretation of the references to color in this figure legend, the reader is referred to the web version of this article.)

cross mark, and adaptive ROI is denoted with red in Fig. 3. Note that the region under the vanishing line (i.e., the vertical coordinate of the vanishing point) establishes the height of the ROI. The ROI for road region can be expressed as follows:

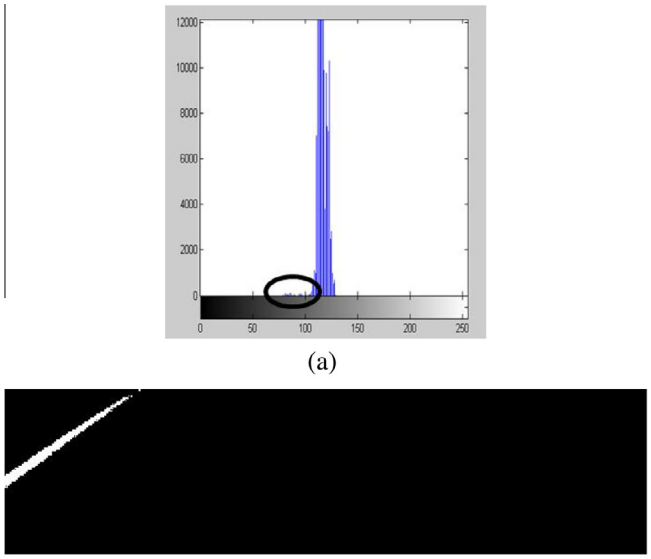

Fig. 7. Yellow lane marker detection: (a) histogram for Cb-component and (b) candidate for yellow lane marker regions.

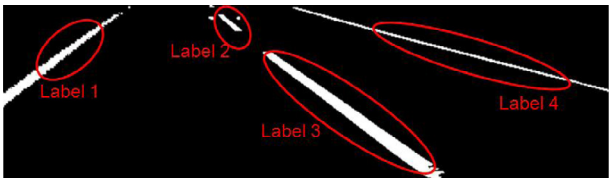

Fig. 8. Lane marker clustering.

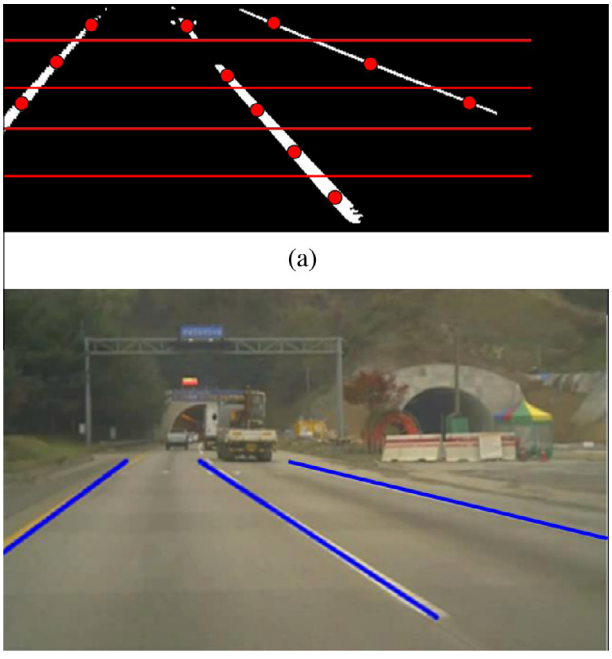

Fig. 9. Lane detection result: (a) lane fitting and (b) lane detection.

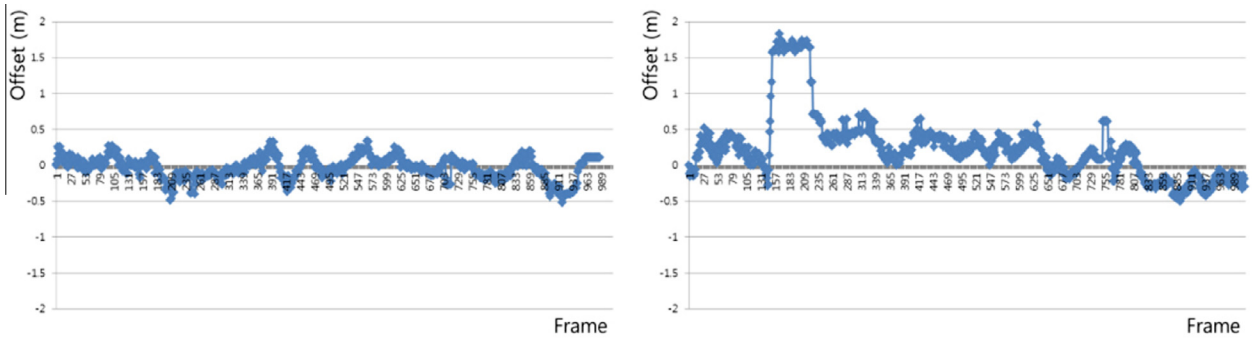

(a) (b)

Fig. 10. Lateral offset: (a) is dataset without lane change and (b) is dataset with lane change.

Table 1
Environment conditions for driving databases.

	Time	Other conditions
DIML's database1 (OV10630)	Day, sunset, sunrise, night	Clear/cloudy/rainy/yellow and white lamps/tunnel
DIML's database2 (Iphone-3gs)	Night	Tunnel/car lamps/light blur/ street lamps
Caltech's database	Day	Urban streets/shadows/curbed streets
SLD 2011's database	Day	Various road mark/highway

$$I_{ROI(x,y)} = \begin{cases} I(x,y), & \text{if } y \leqslant y_{vp} \\ 0, & \text{Otherwise} \end{cases} \tag{1}$$

where y_{vp}, $I(x,y)$ and I_{ROI} are a vertical coordinate of the vanishing point and original image and ROI image, respectively.

3.2. Lane marker detection stage

Lane colors have distinct properties under various illumination conditions, which we utilize to detect the candidates for lane regions. Then, we define the binary lane image by assigning 1 for lane regions and 0 for other regions. In order to make a binary lane image, we convert RGB color values into YCbCr color values, which are suitable for the proposed lane detection method.

3.2.1. White lane marking detection

The white lane in the road image can be defined by the Federal Standard Color #595-17886 (Burdette, 1988), which is equivalent to the RGB value (247,241,227) (http://scalemodeldb.com/). Note that white lanes have a greater probability of having high values, since the value is obtained by $Y = 0.299R + 0.587G + 0.114B$ and all the white lane RGB values are high. In addition, the rank order of the white lane is preserved under illumination changes. R, G, and B values formed at a pixel under a pair of illuminants are related by a diagonal matrix transform as follows:

$$\begin{pmatrix} R^o \\ G^o \\ B^o \end{pmatrix} = \begin{pmatrix} \alpha & 0 & 0 \\ 0 & \beta & 0 \\ 0 & 0 & \gamma \end{pmatrix} \begin{pmatrix} R^c \\ G^c \\ B^c \end{pmatrix} \tag{2}$$

where o and c represent different illumination conditions and α, β and γ are diagonal coefficients which indicate the relationship between o and c illumination conditions (Finlayson, Hordley, Schaefer, & Tian, 2005). The rank order is preserved under the change of illumination and following relation can be derived as follows:

$$\begin{aligned} &R^o = \alpha R^c \\ &R_i^c > R_j^c \rightarrow \alpha R_i^c > \alpha R_j^c, \quad \forall i,j,\ \forall \alpha > 0 \end{aligned} \tag{3}$$

where i and j are coordinates of the image. Y-channel value of white color in YCbCr color space is also applied as follows:

$$\begin{aligned} &Y^c = \alpha Y^o \\ &Y_i^o > Y_j^o \rightarrow \alpha Y_i^o > \alpha Y_j^o, \quad \forall i,j,\ \forall \alpha > 0 \end{aligned} \tag{4}$$

We can confirm from Fig. 4 that Y-channel value for the white color always has the highest value under various illumination conditions compared to other color channels. Thus, we can easily detect white lanes using the above property in YCbCr space. The binary white lane image can be obtained as follows:

$$\begin{aligned} C_y(k) &= \sum_{k=0}^{255} Hist_y(k) \\ B(x,y) &= \begin{cases} 1, & \text{if } C_y(I(x,y)) > T_y \\ 0, & \text{else} \end{cases} \end{aligned} \tag{5}$$

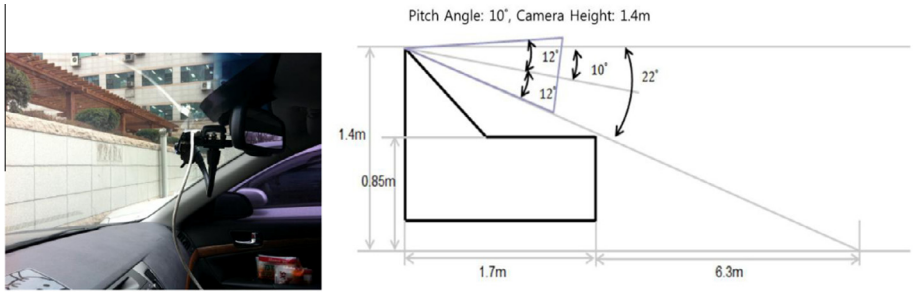

(a) (b)

Fig. 11. Experimental setup: (a) in-vehicle vision sensor system and (b) vision sensor setup configuration.

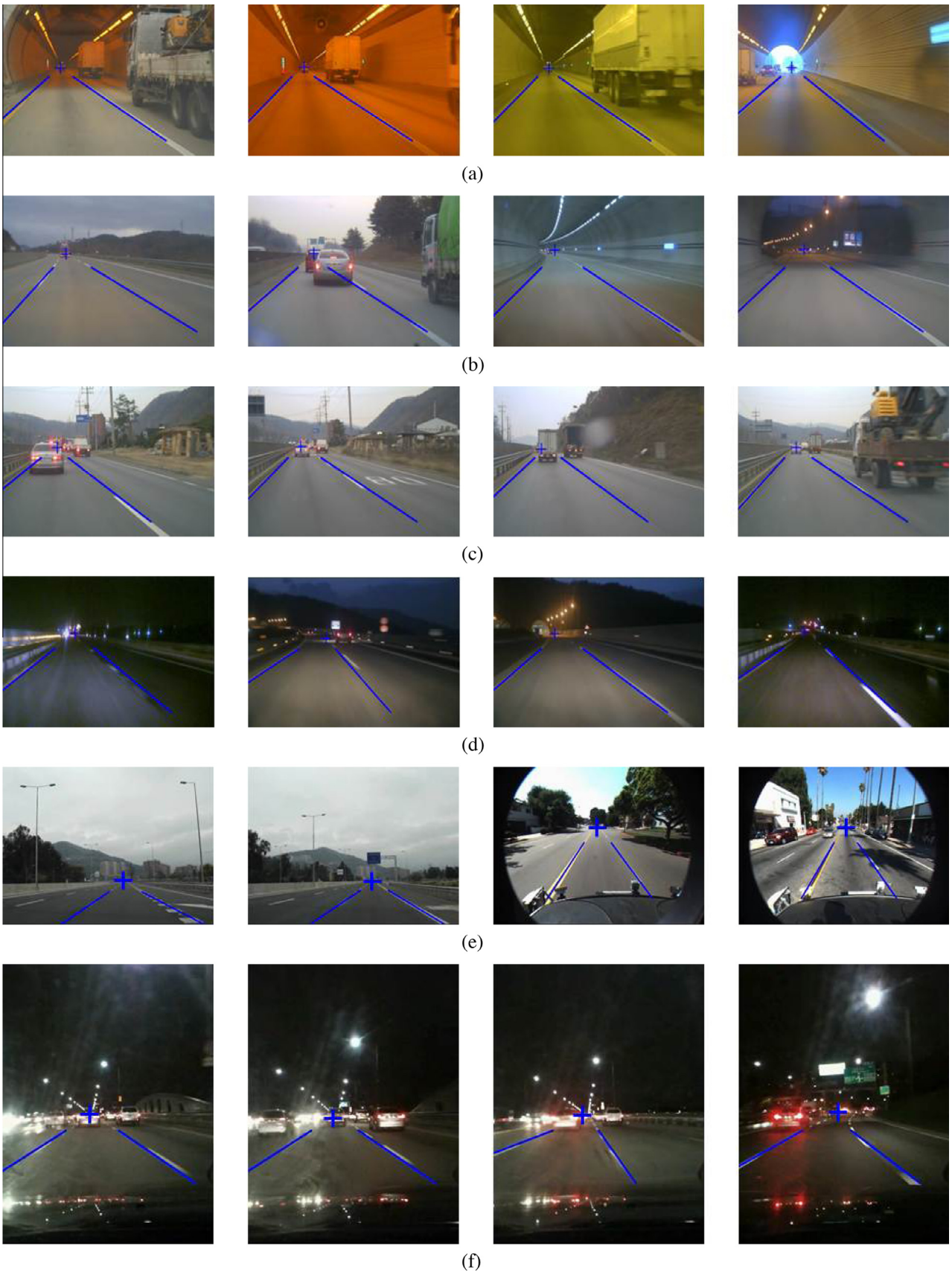

Fig. 12. Lane detection results in various illumination conditions: (a) yellow lamp tunnel, (b) white lamp tunnel and sunrise, (c) sunset and rainy, (d) night, (e) SLD 2011 and Caltech dataset and (f) iPhone dataset. (Detection result videos can be accessed from http://diml.yonsei.ac.kr/jison/LDW). (For interpretation of the references to color in this figure legend, the reader is referred to the web version of this article.)

where $C_y(k)$, $Hist_y(k)$, $B(x,y)$, k and T_y are the cumulative histogram, histogram, white binary image, intensity and Y-component threshold, respectively. We empirically set T_y to 0.97 (top 3%) since the pixels of the white lane typically occupy 3–5% of the road image structure as shown in Fig. 5; White lane area corresponds to the region of the black circle in Fig. 5(a).

3.2.2. Yellow lane marking detection

The yellow lane in the road image can be defined by Federal Standard Color #595-33538 (Burdette, 1988), which is equivalent to the RGB value (255,183,0) (http://scalemodeldb.com/). Yellow lanes have smaller values since the value is obtained by $Cb = -0.169R - 0.331G + 0.5B + 128$ and R and G values of the yellow lane are high while the B value is 0. Thus, the color of the yellow lane is only dependent on the R and G values. We can confirm from Fig. 6 that Cb-channel value for the yellow color always has the lowest value under various illumination conditions compared to other color channels. Thus, we can easily detect yellow lanes using the above property in YCbCr space. The binary yellow lane image can be obtained as follows:

$$C_{cb}(k) = \sum_{k=0}^{255} Hist_{cb}(k)$$
$$B(x,y) = \begin{cases} 1, & \text{if } C_{cb}(I(x,y)) < T_{cb} \\ 0, & \text{else} \end{cases} \quad (6)$$

where $C_{cb}(k)$, $Hist_{cb}(k)$, $B(x,y)$, k and T_{cb} are the cumulative histogram, histogram, white binary image, intensity and Cb-component threshold, respectively. We empirically set T_{cb} to 0.01 (low 1%) since the pixels of the yellow lane typically occupy 1–3% of the road image structure as shown in Fig. 7; Yellow lane area corresponds to the region of the black circle in Fig. 7(a).

3.3. Lane clustering and fitting stage

The binary lane image is obtained by combining the binary white and yellow lane images using OR operation. We use the connected component clustering method (Rudra, Shahanaz, Subhadi, & Radhakrishna, 2009) in binary lane image since lanes have connecting property. Each label is divided as shown in Fig. 8. We extract the center coordinate values in each label. We calculate the label's angle and the intercept of y-axis. If the labels have similar angle and intercept values of y-axis, they are combined to make one region to form a cluster.

We divide an image into 5 sections, each section represents equidistance from the vehicle as shown in Fig. 9(a). In each section, we extract a center point from each cluster. Extracted points in each cluster make one line by using least squares line fitting algorithm as shown in Fig. 9(b). We detect a main lane, which could be one left and one right lane, based on the number of clustering model's binary pixels as well as the length of the detected line.

3.4. Lane departure warning stage

We measure temporal variations of lane offset and lane mark heading angle to detect lane departure. Fig. 10(a) shows offset variance without lane change. Fig. 10(b) shows offset variance with lane change. Road width of a lane in our database is 3 meter. If offset variance is larger than 1.5 (m), we consider it as lane departure situation as shown in Fig. 10(b) and send alarm signal.

4. Experimental results

The dataset in various illumination and environmental conditions is needed to evaluate vision-based ADAS. Since the performance of a vision-based method varies according to illumination changes, we consider illumination conditions for constructing the dataset. Illumination changes in road environments may include natural light changes and artificial light changes. Natural light changes are caused by time and weather, and artificial light changes are caused by the characteristics of streetlamps and vehicle lamps. Road type is another important factor in developing ADAS. Also, The performance is influenced by the types of devices. Thus, we created driving scenarios considering these factors as shown in Table 1. DIML's database1 used an OV10630 image sensor, which provides 1280×800 resolution at 15 frames per second. The sensor is mounted behind the rearview mirror as shown in Fig. 11(a). The camera configuration is depicted in Fig. 11(b). For two months, we constructed the database in downtown and urban roads of Korea (Yoo et al., 2013). DIML's database2 used an iPhone which provides 480×640 resolution images at 30 frames per second. Since SLD 2011 and Caltech dataset (Aly, 2008) are public datasets, we used them for objective evaluation. Since Various datasets include various situations such as traffic, pedestrians, and obstacles, they can be used to develop and evaluate various vision-based ADAS and lane detection methods.

Fig. 12 shows lane detection results with the proposed method for several road image sequences under various illumination conditions. The video results for lane detection can be found in http://diml.yonsei.ac.kr/jison/LDW. The detection rate was strictly measured via visual inspection by a single user. The following rules were used to quantify the results into three categories: (i) correct detection, in which more than 70% of the estimated lane markers were overlaid on a lane in the scene; (ii) incorrect detection, in which the estimated lane marker was overlaid on the other area;

Table 2
Lane detection rate of the proposed algorithm in various environments.

			Detection rate (%)	Time (ms/frame)
DIML-1 (5230 frame)	Sunset (750 frame)		96	33
	Day tunnel (1000 frame)	Entering	83.5	34.1
		Inside	93.2	
		Exiting	86.7	
	Day rainy (1300 frame)		89	33.2
	Sunrise (900 frame)		92	32
	Night tunnel (790 frame)	Entering	91.3	34.5
		Inside	98.1	
		Exiting	94.2	
	Night rainy (490 frame)		93	32.1
DIML-2 (3000 frame)	Night (3000 frame)		94.3	36.2
Caltech (569 frame)	Day urban (569 frame)		93.6	31.2
SLD 2011 (1437 frame)	Day highway (1437 frame)		94.2	36.4
Average	Total image (10236 frame)		93.4	34.5

Fig. 13. Examples of false-detection and miss-detection results: (a) lane-like crack, (b) partially occluded lane mark and low sun angle situations, (c) blur lane marks at night and (d) blur lane marks under rainy weather.

and (iii) missed, in which estimation failed when a lane was visible. The detection rate is calculated as follows:

$$DR = \frac{C}{N} \times 100(\%) \tag{7}$$

where DR, C and N denote the detection rate, the number of correctly detected frames, and the number of total frames, respectively. The average detection rate from 10,236 frames was 93% as summarized in Table 2. We confirmed that the performance of the proposed lane detection method was not largely affected by illumination changes. In addition, the overall process required only 33 ms per frame and thus, it can be used for real-time applications. Even though the proposed lane detection algorithm works well enough for several Datasets, which include various illumination conditions, it still has some unsolved problems such as lane-like crack, partially occluded lane mark, blur lane marks, etc. Fig. 13 shows some examples of false-detection and miss-detection results with the proposed method.

5. Conclusion

In this paper, we focused on handling illumination problem which is important in driving environment. Although it has some limitations in challenging scenarios such as blur lane marks and low sun angle situations, the proposed method shows stable detection performance under various illumination conditions.

Conventional lane detection methods provide unstable performance under various illuminations and have high computational complexities. Even though they work well in very well-controlled environments, they may fail under difficult conditions such as in bad weathers and at night time. In addition, it may cause serious problems if they do not work in real-time under dynamically changing outdoor traffic environments.

To solve the above problems, we reduced the computational complexity by detecting a vanishing point and establishing an adaptive ROI. We then detected lanes using invariance properties of lane colors under various illumination conditions. Thus, the proposed method gives better detection performance for various datasets that we tested and it is suitable to implement real-time ADAS. Experimental results of the proposed method showed an average detection rate of 93% under various illumination conditions with an execution time of 33 ms, which is sufficiently fast for real-time applications and lane departure warning system.

Even though the proposed method is invariant against various illumination changes, it is still difficult to handle several extreme conditions such as strong light reflection, blur lane marks, low sun angle situations and lane cracks. These extreme conditions may make lane marks being disappeared in captured images and it makes vision-based lane detection very difficult.

To overcome the above limitations of vision-based lane detection methods, we should study further for the efficient combination of other ADAS including multi-modal sensor data. Other modality data obtained by various multispectral imaging sensors may be used together with RGB data to solve many problems which cannot be overcome by our proposed method. For example, Near Infrared (NIR) image can help solving the saturation problem of vision sensor caused by strong reflections.

Acknowledgment

This work was supported by the National Research Foundation of Korea (NRF) Grant funded by the Korea government (MSIP) (NRF-2013R1A2A2A01068338).

References

Aly, M. (2008). Real time detection of lane markers in urban streets. In *IEEE intelligent vehicles symposium*.

Borkar, A., Hayes, M., & Smith, M. (2012). A novel lane detection system with efficient ground truth generation. *IEEE Transactions on Intelligent Transportation Systems, 13*(1), 365–374.

Burdette, E. G. (1988). National cooperative highway research program report 306 transportation research board. National research (p. 40).

Cannny, J. (1986). A computational approach to edge detection. *IEEE Transactions on Pattern Analysis and Machine Intelligence, 8*(6), 679–698.

Chin, K. Y., & Lin, S. F. (2005). Lane detection using color-based segmentation. In *IEEE intelligent vehicles symposium* (pp. 706–711).

David, F. M., Jose, G. P., Pablo, A. G., & Mateo, B. G. (2012). Vehicular traffic surveillance and road lane detection using radar interferometry. *IEEE Transactions on Vehicular Technology, 61*(3), 959–970.

Finlayson, G. D., Hordley, S. D., Schaefer, G., & Tian, G. Y. (2005). Illuminant and device invariant colour using histogram equalisation. *IEEE Transactions on Pattern Analysis and Machine Intelligence, 38*(2), 179–190.

Foedisch, M., & Takeuchi, A. (2004). Adaptive real-time road detection using neural networks. In *IEEE conference on intelligent transport system* (pp. 167–172).

Glaser, S., Mammar, S., & Sentouh, C. (2010). Integrated driver-vehicle-infrastructure road departure warning unit. *IEEE Transactions on Vehicular Technology, 59*(6), 2757–2771.

Graovac, S., & Goma, A. (2012). Detection of road image borders based on texture classification. *International Journal of Advanced Robotic Systems, 9*, 1.

Hsiao, P. Y., Yeh, C. W., Huang, S. S., & Fu, L. C. (2006). A portable real-time lane departure warning system based on embedded calculating technique. *IEEE Transactions on Vehicular Technology*, 2982–2986.

Kang, S., Lee, S., Hur, J., & Seo, S. (2014). Multi-lane detection based on accurate geometric lane estimation in highway scenarios. In *IEEE intelligent vehicles symposium*.

Kong, H., Audibert, J. Y., & Ponce, J. (2010). General road detection from a single image. *IEEE Transactions on Image Processing, 19*(8), 2211–2220.

Kuk, J. G., An, J. H., Ki, H., & Cho, N. I. (2010). Fast lane detection & tracking based on hough transform with reduced memory requirement. In *IEEE conference on intelligent transportation systems* (pp. 1344–1349).

Leandro, A. F. F., & Manuel, M. O. (2008). Real-time line detection through an improved hough transform voting scheme. *Pattern Recognition, 41*(1), 299–314.

Mccall, J. C., & Trivedi, M. M. (2006). Video-based lane estimation and tracking for driver assistance survey system and evaluation. *IEEE Transactions on Intelligent Transportation Systems, 7*(1), 20–37.

Rudra, N. H., Shahanaz, S., Subhadi, B., & Radhakrishna, P. (2009). A simple and efficient lane detection using clustering and weighted regression. In *International conference on management of Data COMAD*.

Sotelo, M., Rodriguez, F., Magdalena, L., Bergasa, L., & Boquete, L. (2004). Color vision-based lane tracking system for autonomous driving in unmarked roads. *Autonomous Robots, 16*(1), 95–116.

Southhall, J. B., & Taylor, C. (2001). Stochastic road shape estimation. In *Proceedings of the IEEE international conference on computer vision* (pp. 205–212).

Sun, T. Y., Tsai, S. J., & Chan, V. (2006). HSI color model based lane-marking detection. In *IEEE conference on intelligent transport system* (pp. 1168–1172).

Wang, J.-G., Lin, C.-J., & Chen, S.-M. (2010). Applying fuzzy method to vision-based lane detection and departure warning system. *Expert Systems with Applications, 37*(1), 113–126.

Yoo, H., Yang, U., & Sohn, K. (2013). Gradient-enhancing conversion for illumination-robust lane detection. *IEEE Transactions on Intelligent Transportation Systems, 14*(3), 1083–1094.

Youchun, X., Rongben, W., et al. (2001). A summary of worldwide intelligent vehicle. *Automotive Engineering, 23*(5), 289–295.